forests

MDPI

Article

An Effect of Urban Forest on Urban Thermal Environment in Seoul, South Korea, Based on Landsat Imagery Analysis

Peter Sang-Hoon Lee [1] **and Jincheol Park** [2,*]

[1] Graduate School of Urban Studies, Hanyang University, Seoul 04763, Korea; peter337@hanyang.ac.kr
[2] Seoul Industry-University-Research Cooperation Foundation, Hanyang University, Seoul 04763, Korea
* Correspondence: jincheol90@gmail.com

Received: 30 April 2020; Accepted: 28 May 2020; Published: 2 June 2020

Abstract: The urban heat island effect has posed negative impacts on urban areas with increased cooling energy demand followed by an altered thermal environment. While unusually high temperature in urban areas has been often attributed to complex urban settings, the function of urban forests has been considered as an effective heat mitigation strategy. To investigate the cooling effect of urban forests and their influence range, this study examined the spatiotemporal changes in land surface temperature (LST) of urban forests and surrounding areas by using Landsat imageries. LST, the size of the urban forest, its vegetation cover, and Normalized Difference Vegetation Index (NDVI) were investigated for 34 urban forests and their surrounding areas at a series of buffer areas in Seoul, South Korea. The mean LST of urban forests was lower than that of the overall city, and the threshold distance from urban forests for cooling effect was estimated to be roughly up to 300 m. The group of large-sized urban forests showed significantly lower mean LST than that of small-sized urban forests. The group of urban forests with higher NDVI showed lower mean LST than that of urban forests with lower mean NDVI in a consistent manner. A negative linear relationship was found between the LST and size of urban forest ($r = -0.36$ to -0.58), size of vegetation cover ($r = -0.39$ to -0.61), and NDVI ($r = -0.42$ to -0.93). Temporal changes in NDVI were examined separately on a specific site, Seoul Forest, that has experienced urban forest dynamics. LST of the site decreased as NDVI improved by a land-use change from a barren racetrack to a city park. It was considered that NDVI could be a reliable factor for estimating the cooling effect of urban forest compared to the size of the urban forest and/or vegetation cover.

Keywords: urban forest; urban heat island; land surface temperature (LST); thermal environment; remote sensing; Landsat imagery; vegetation index; landscape analysis

1. Introduction

The urban heat island (UHI) effect describes an urbanization-driven phenomenon where the ambient temperature is higher in built-up areas than surrounding rural areas particularly at night. It can result from a variety of different urban settings including anthropogenic influence, microclimate, and geographical and environmental factors, similar to other urban issues [1–4]. As rapid and steady urban growth is expected to take place in many cities over the world, there are concerns that the UHI effect is one of the major factors that negatively affect the current global warming trend, followed by the increased cooling energy consumption [5–7]. In response to the ongoing situation, there have been extensive efforts to identify the role of urban forests in mitigating the UHI effect. Urban forests are an assemblage of a variety of tree species, which can meteorologically affect the thermal environment in urban areas by providing a divergent outflow of cool air toward surrounding areas at surface level and replacing the hotter surfaces of urban features such as buildings and roadways with green canopies [1,8]. Such beneficial functions expected from the presence of urban forests can become less effective when urban forests are replaced with or disturbed by urban features over time. Mitigation performances of tree species on cooling surface temperature may change during and after disturbance occurred by anthropogenic activities, and urban forests can be more susceptible to such changes due to their location particularly in urban settings.

There have been several attempts to investigate the thermal environment of urban forests over a vast area. The relationships among land surface temperature (LST), vegetation abundance, and land-use type were investigated at the city-scale with the use of satellite imagery. For example, a negative relationship was found between LST and vegetation abundance estimated using a series of vegetation indices was presented [9]; and LST was lower in the areas containing higher area proportion of forests and semi-natural areas [10]. The relationships among the LST and characteristics of urban forests such as forest patch size and area proportion of green space at a city scale based upon a single satellite imagery per sample site were also examined [11,12]. A negative correlation was found between the urban forest park size and LST estimated by using two different satellite data [11], and a negative correlation was found between the percent cover of green space in the city and the LST by using a series of satellite data with different sensor resolutions [12]. Despite many community- and/or local-scale studies on the cooling effect of an urban forest on its neighboring area, it is still challenging to understand such effects on a larger scale due to lack of meteorological data and detailed information on the urban forest area. Since weather stations are limited fundamentally in number and also in the diversity of location, primarily focusing on representative urban areas with high population [13], the data availability to investigate thermal environment in and/or around urban forests such as ambient temperature and LST generally relies on field observation conducted by individual researchers. To overcome this limitation, remote sensing-based approaches to performing landscape-scale temperature mapping have been developed. For instance, thermal band data retrieved from satellites have been used for estimating LST over a large area in the use of a series of different algorithms [9,10,14–20].

Employing the temperature mapping algorithms suggested in earlier studies, this study concentrated on identifying the spatiotemporal changes in LST over urban forests and their adjacent area in the city of Seoul, South Korea. The objectives of this study were: (i) investigating the cooling effect of urban forest on its surrounding area (ii), identifying vegetation characteristics of urban forests which could be related to the cooling effect of urban forests, and (iii) examining temporal changes in the thermal environment from urban forest characteristics.

2. Materials and Methods

2.1. Study Area

The study area included urban forests distributed across Seoul, South Korea. Seoul is one of the megacities that have been experiencing rapid urbanization and is currently the most populated metropolis in South Korea with approximately 10 million inhabitants in 600 km^2 in area. This has been followed by high population density and the city is a highly developed setting which has led to increasing concerns and efforts, such as green initiatives, to mitigate the UHI effect on the city [21,22]. The landscape of Seoul consists of a complex assortment of urban surfaces and features, mountains and natural forests, and green infrastructure including flattened and hilly urban forests, parks, and open green spaces [23,24]. A suite of urban forests was selected as the samples in this study, considering size and characteristics of the surrounding environment as well as topographical features of the urban forest. Urban forests located on relatively flat surfaces were counted as samples to exclude the effect of topographical setting. A group of urban forests connected to big mountainous forests and/or water bodies was excluded to avoid the influence of additional natural environments. Simultaneously, urban forests smaller than 2 ha in the area were also out of the scope of this study due to their insufficient characteristics as urban forest in general [25]. One of the urban forests, Seoul Forest, was used for reviewing its time-series changes because of its recent creation during our study period. Spatial information such as locations of urban forests and land-use of Seoul was obtained from the Korean Ministry of the Interior and Safety [26] and Seoul Metropolitan Government [27]. The samples selected from the urban forests in this study area were delineated in Figure 1 and listed in Table 1 subsequently.

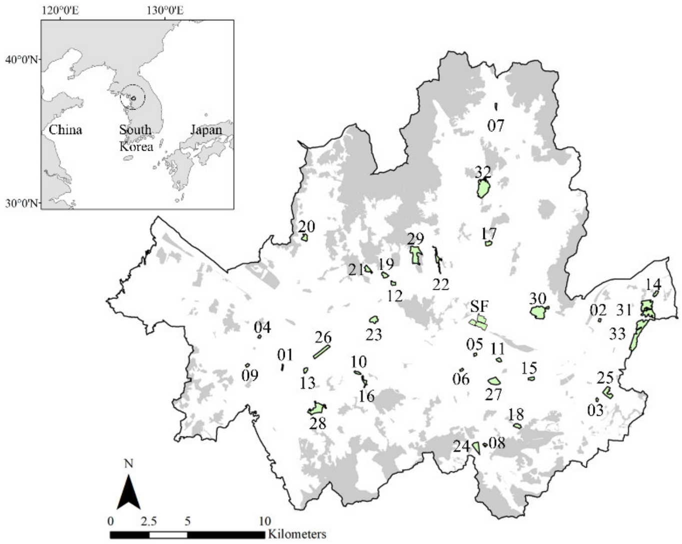

Figure 1. Distribution of the Seoul's urban forests of which sizes are larger than 2 ha in area (in shade) and the selected urban forests as samples (in green and red) in this study; the samples are numbered in the order of size from the smallest (no. 01) to the largest (no. 33); the sample named "SF" indicates where a separate case study is conducted.

Table 1. Code, name, and size of the 33 selected urban forests in the study area coded in the size order from the smallest urban forest (UF 01) to the largest (UF 33), and the separate case study area of "SF".

Code	Name	Area (ha)	Code	Name	Area (ha)
UF 01	Mullae neighborhood park	2.5	UF 18	Gaepo park	9.8
UF 02	Cheonho park	2.7	UF 19	Gyeonghuigung palace	9.8
UF 03	Garak neighborhood park	2.8	UF 20	Sinsa neighborhood park	11.0
UF 04	Paris park	3.0	UF 21	Seodaemun independence park	11.3
UF 05	Dosan park	3.0	UF 22	Naksan park	15.4
UF 06	Hak-dong park	3.0	UF 23	Hyochang park	16.1
UF 07	Sanggye neighborhood park	3.0	UF 24	Yangjae citizen's forest	18.3
UF 08	Yangjae neighborhood park	3.3	UF 25	Ogeum park	21.9
UF 09	Yangcheon park	3.4	UF 26	Yeouido park	22.6
UF 10	Sayuksin park	4.9	UF 27	Seojeongneung	24.1
UF 11	Cheongdam Park	5.9	UF 28	Boramae park	41.5
UF 12	Deoksugung Palace	6.1	UF 29	Changdeokgung park	46.8
UF 13	Yeongdeungpo Park	6.2	UF 30	Seoul children's grand park	60.8
UF 14	Dongmyeong neighborhood park	6.5	UF 31	Myeongil park	64.4
UF 15	Asia neighborhood park	6.6	UF 32	North Seoul dream forest	66.5
UF 16	Gogu dongsan	8.0	UF 33	Gil-dong eco park	70.8
UF 17	Hongneung neighborhood park	9.6	UF SF	Seoul Forest	54.8

2.2. Urban Forest Buffer and Land Use Land Cover (LULC)

To identify an influence range of each urban forest, the surrounding area from an individual sample was divided by distance [28]. At each sample, domains were designed by being given four distance groups from the outer boundary of each, which was called a "buffer" in this study: 0 to 100 m ($Buffer_{100}$), 100 to 300 m ($Buffer_{300}$), 300 to 500 m ($Buffer_{500}$), and 500 to 1000 m ($Buffer_{1000}$) (Figure 2).

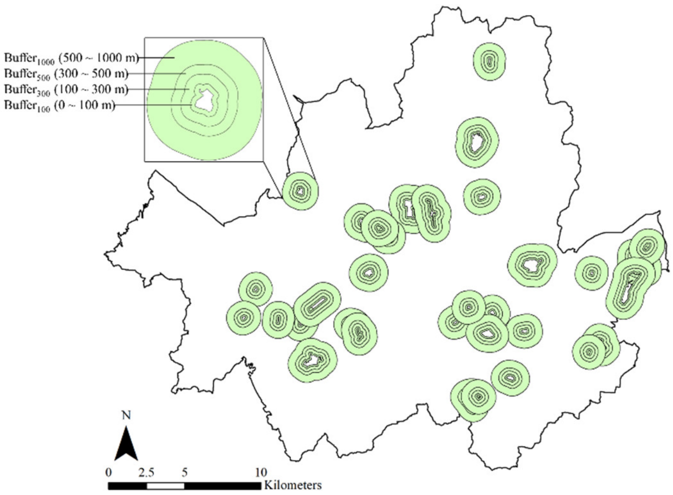

Figure 2. Distributions of the 33 samples of urban forest and their buffers of 0 to 100 m (Buffer$_{100}$), 100 to 300 m (Buffer$_{300}$), 300 to 500 m (Buffer$_{500}$), and 500 to 1000 m (Buffer$_{1000}$).

To investigate the changes in thermal environment with different urban settings, nearby urban forests, the land use and land cover (LULC) information at each domain was quantified. The LULC data was obtained from the Seoul Metropolitan Government [27].

2.3. Data Collection and Processing

2.3.1. Satellite-Borne Data

LST over the whole study area was estimated with the use of satellite-borne imagery. Temporal changes in LST over the study area were investigated by two separate seasons of summer and winter from 2002 to 2019, using a series of images with its cloud cover less than 10%. Landsat 5 Thematic Mapper (TM) Collection 1 Level-1 data products (LT05_L1XX) and Landsat 8 Operational Land Imager and Thermal Infrared Sensor (OLI/TIRS) Collection 1 Level-1 data products (LC08_L1XX) in 30 m sensor resolution were downloaded from the USGS online data archive [29]. The acquisition times of Landsat 5 and 8 images were approximately 02:00 UTC (11:00 AM in Korean local time) only when the satellite overpasses the study area. The information on the imagery is explained in Table 2.

Table 2. Acquisition information of the Landsat 5 and 8 images used in this study.

No.	Date (yyyymmdd)	Season	File no.	Sensor
1	20020630	Summer	LT05_L1TP_116034_20020630_20161207_01_T1	Landsat 5 TM
2	20030108	Winter	LT05_L1TP_116034_20030108_20161206_01_T1	Landsat 5 TM
3	20040603	Summer	LT05_L1TP_116034_20040603_20161201_01_T1	Landsat 5 TM
4	20050113	Winter	LT05_L1TP_116034_20050113_20161127_01_T1	Landsat 5 TM
5	20090601	Summer	LT05_L1TP_116034_20090601_20161025_01_T1	Landsat 5 TM
6	20091124	Winter	LT05_L1TP_116034_20091124_20161022_01_T1	Landsat 5 TM
7	20150704	Summer	LC08_L1TP_116034_20150704_20170407_01_T1	Landsat 8 OLI/TIRS
8	20151227	Winter	LC08_L1TP_116034_20151227_20170331_01_T1	Landsat 8 OLI/TIRS
9	20190613	Summer	LC08_L1TP_116034_20190613_20190619_01_T1	Landsat 8 OLI/TIRS
10	20191206	Winter	LC08_L1TP_116034_20191206_20191217_01_T1	Landsat 8 OLI/TIRS

2.3.2. Land Surface Temperature (LST) Modeling

In order to retrieve the estimated LST, multispectral data retrieved at band 3 (red), 4 (near-infrared (NIR)), and 6 (thermal) from Landsat 5 images, and band 4 (red), 5 (near-infrared), and 10 (thermal) from Landsat 8 images were pre-processed according to the following steps including improved mono-window algorithm: (i) the pixel values of thermal bands were converted to Top of Atmospheric (TOA) spectral radiance [14,30,31], (ii) the TOA spectral radiance was converted to at-sensor temperature [9,15,31], (iii) the pixel values of visible bands (red) and near-infrared (NIR) bands were used to calculate Normalized Difference Vegetation Index (NDVI) (See Section 2.3.3), (iv) the proportion of vegetation was calculated by using the NDVI [16,17,32,33], (v) the land surface emissivity was computed by using NDVI Thresholds Method [16,18,30], and (vi) the emissivity-corrected LST was calculated [9,10,19,20,30,34]. Temperature maps modeled in this procedure were used to estimate the LST of each urban forest and its surrounding area, considering mean LST on each site as the representative value regardless of size and environmental conditions of the spot.

2.3.3. Green Patch Analysis

To evaluate the vegetation status of each urban forest by estimating the vegetation greenness based upon spatial information and remotely sensed data, a tree-covered area called a green patch in this study was extracted from the individual urban forest. Green patch size in the area was computed by using NDVI employed as the indicator of vegetation greenness, healthiness, and/or density of urban forest [35] with the following fundamental formula:

$$\mathrm{NDVI} = (\mathrm{NIR}-\mathrm{R})/(\mathrm{NIR} + \mathrm{R}) \quad (1)$$

where NIR is the value of near-infrared of the surface reflectance from Landsat imagery, and R is the red value [35,36]. Due to two different data sets providing different settings of spectral resolution, the equations used for NDVI retrieval in this study were distinguished as follows:

$$\mathrm{NDVI\ (Landsat\ 5)} = (\mathrm{Band\ 4}-\mathrm{Band\ 3})/(\mathrm{Band\ 4} + \mathrm{Band\ 3}) \quad (2)$$

$$\mathrm{NDVI\ (Landsat\ 8)} = (\mathrm{Band\ 5}-\mathrm{Band\ 4})/(\mathrm{Band\ 5} + \mathrm{Band\ 4}) \quad (3)$$

where Bands 3 and 4 in Equation (2) are retrieved from Landsat 5 dataset and Bands 4 and 5 in Equation (3) are from Landsat 8 dataset with no atmospheric correction due to the imageries' single-scene coverage having marginal differences in atmospheric information between the scenes [18,30,37]. The mean NDVI computed on the area each urban forest was assigned to each sample. The software ArcMap version 10.2 (ESRI, Redlands, California) was used for the data processing on green patch size and NDVI.

2.4. Statistical Analysis

To investigate the cooling effect of an urban forest on its surrounding area, the mean LST of the urban forest sample and its neighboring buffers were compared to each other. To identify the factors that could affect the cooling capacity of the urban forest, correlations analyses were conducted between size in area and NDVI of each sample and land-use type of the surrounding area. Comparative analyses including one-way ANOVA analysis were conducted between the temporal changes in mean LST of the group of large-sized urban forests and their buffers and the group of small-sized urban forests and their buffers. All statistical analyses were performed by using the software SPSS Statistics 25 (International Business Machines, Armonk, New York, NY, USA).

3. Results

To examine the cooling effect of an urban forest on its surrounding area, the LSTs of the individual samples of urban forests and their buffers were plotted, using the data from 13 June 2019 data as an example (Figure 3).

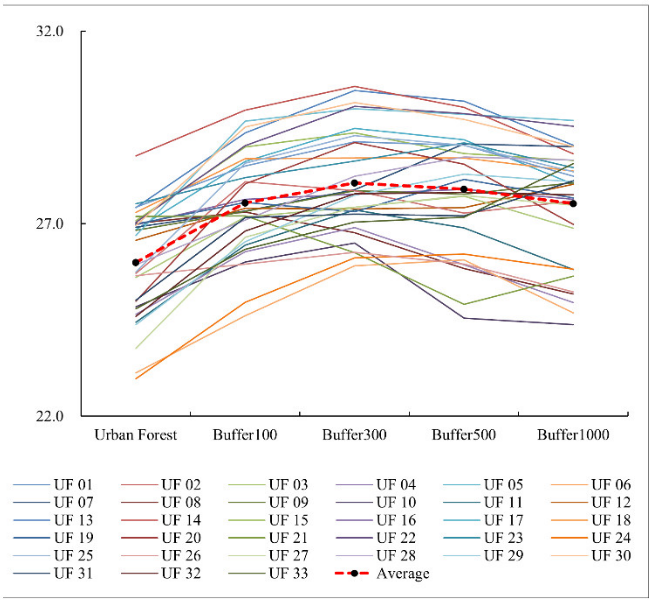

Figure 3. Mean land surface temperatures (LSTs) for the individual urban forests and their $Buffer_{100}$, $Buffer_{300}$, $Buffer_{500}$, and $Buffer_{1000}$ (solid line) and of the entire urban forests and their buffers (dotted line) on 13 June 2019 in the study area, Seoul.

The mean LSTs for most urban forests tended to get higher with the distance from themselves up to 300 m, and then become lower after the distance of 300 m (Figure 3). Such a trend was also found in time-series analysis on the changes in the annual mean LST of the suites of urban forests and their buffers during the study period of 2002 to 2019, yet only in summer (Figure 4).

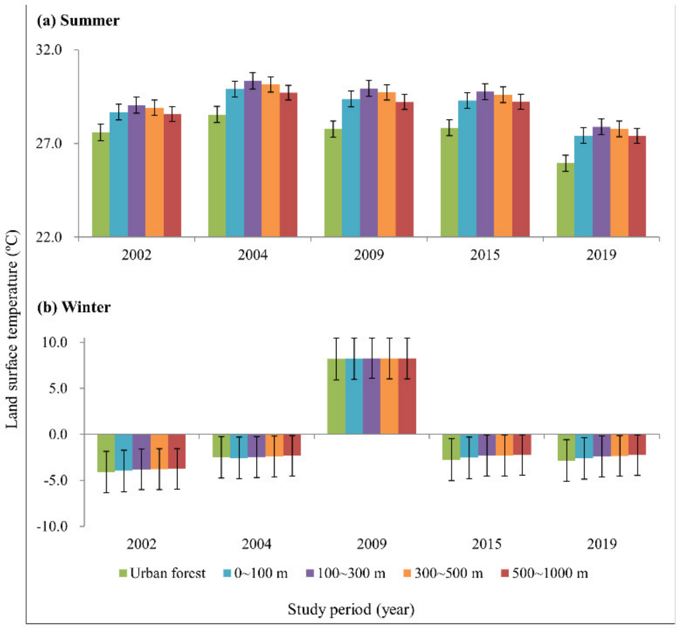

Figure 4. Mean surface temperatures (LSTs) of the selected urban forests and their $Buffer_{100}$, $Buffer_{300}$, $Buffer_{500}$, and $buffer_{1000}$ and standard errors in (**a**) summer seasons and (**b**) winter seasons in the study area, Seoul.

Unlike the clear pattern in summer, there was no noticeable trend found in winter (Figure 4b); therefore, further analyses were focused on the summer season after this point. The mean LSTs increased sequentially up to 300 m from the urban forests and then decreased with distance after 300 m from the urban forests (Figure 4). According to the pattern, the influence range of the cooling effect of the urban forest was decided to reach the $Buffer_{300}$ in this study.

Regarding the LST changes in some urban forests shown in Figure 3, which deviated from the general trend, it was considered that there might be a certain property in the urban forest that is strongly related to the cooling capacity against its surrounding area. To identify the significant factor for the cooling effect, land use over buffer regions of urban forests was investigated. The size in the area of each land use was computed, and correlation analysis was conducted between the LST, the size of the urban forest and green patch, NDVI over urban forest, and area proportion of each land use by $Buffer_{100}$ or $Buffer_{300}$ showing the outcome in Table 3.

Table 3. Pair-wise correlations between the variables from the selected urban forests and their $Buffer_{100}$ and $Buffer_{300}$.

Dependent Variable	Independent Variable			
	Temp [a]	UF [b]	Green [c]	NDVI [d]
100 Temp [e]	0.86 *	−0.31 *	−0.34 *	−0.52 *
300 Temp [f]	0.74 *	−0.23 *	−0.26 *	−0.41 *

*: $p \leq 0.05$. [a]: Mean land surface temperature (LST) of urban forests in this study [b,c,d]: Mean urban forest size, green patch size, and Normalized Difference Vegetation Index (NDVI) of the urban forest [e,f]: Mean LST at $Buffer_{100}$ and $Buffer_{300}$ of the urban forests.

In terms of mean LST, the correlation was stronger between urban forests and their $Buffer_{100}$ ($r = 0.86$, $p \leq 0.05$) than their $Buffer_{300}$ ($r = 0.74$, $p \leq 0.05$), which indicated that the areas in closer proximity to urban forests could be more advantageous for mitigating high LST. As for urban forest size, green patch size, and NDVI, they presented stronger correlations with the mean LST of $Buffer_{100}$ than those of $Buffer_{300}$ (Table 3). It was estimated that the influence range of the cooling effect of urban forests, which supported the general pattern of summer LST in Figure 4a, might not go much farther than 300 m. Based upon the result from correlation analysis (Table 3), the outputs from investigating the relationships between the LST, urban forest size, and green patch size are shown in Figure 5.

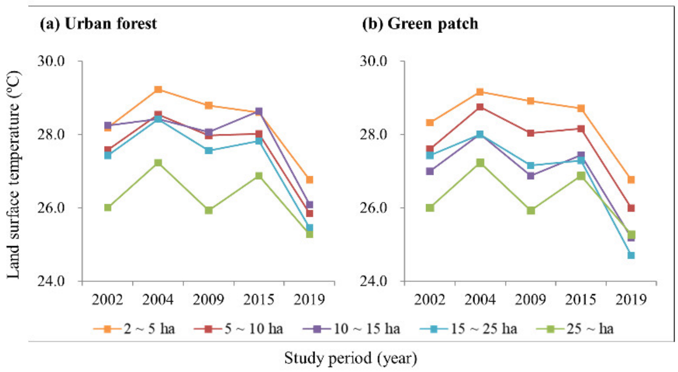

Figure 5. Temporal changes in summer land surface temperature (LST) through the study period for the selected urban forests in the series of size groups: 2 to 5 ha, 5 to 10 ha, 10 to 15 ha, 15 to 25 ha, and over 25 ha (**a**) urban forest size and (**b**) green patch size.

The temporal changes in the mean LSTs of the urban forests in five different size groups were distinguished in Figure 5. The pattern of urban forests (Figure 5a) was also compared with the green patch (Figure 5b) by size in area. Overall, the mean LST was lower where the urban forest size was larger (Figure 5a), and a similar tendency was found between the mean LST and green patch size within the urban forest (Figure 5b). The LSTs tended to be lowest in both the largest urban forest size group and the largest green patch size group, and to be highest in both the smallest urban forest group and the smallest green patch group in a given time. Among the in-between sizes, however, the LST changed differently over time between the urban forest and green patch by size (Figures 5). Hence, because each urban forest has a different proportion of green patch within it, correlation analysis was conducted between the LST and the size of an urban forest and green patch, respectively, in order to identify which variable between urban forest and green patch sizes could be more influential on the thermal environment (Figure 6).

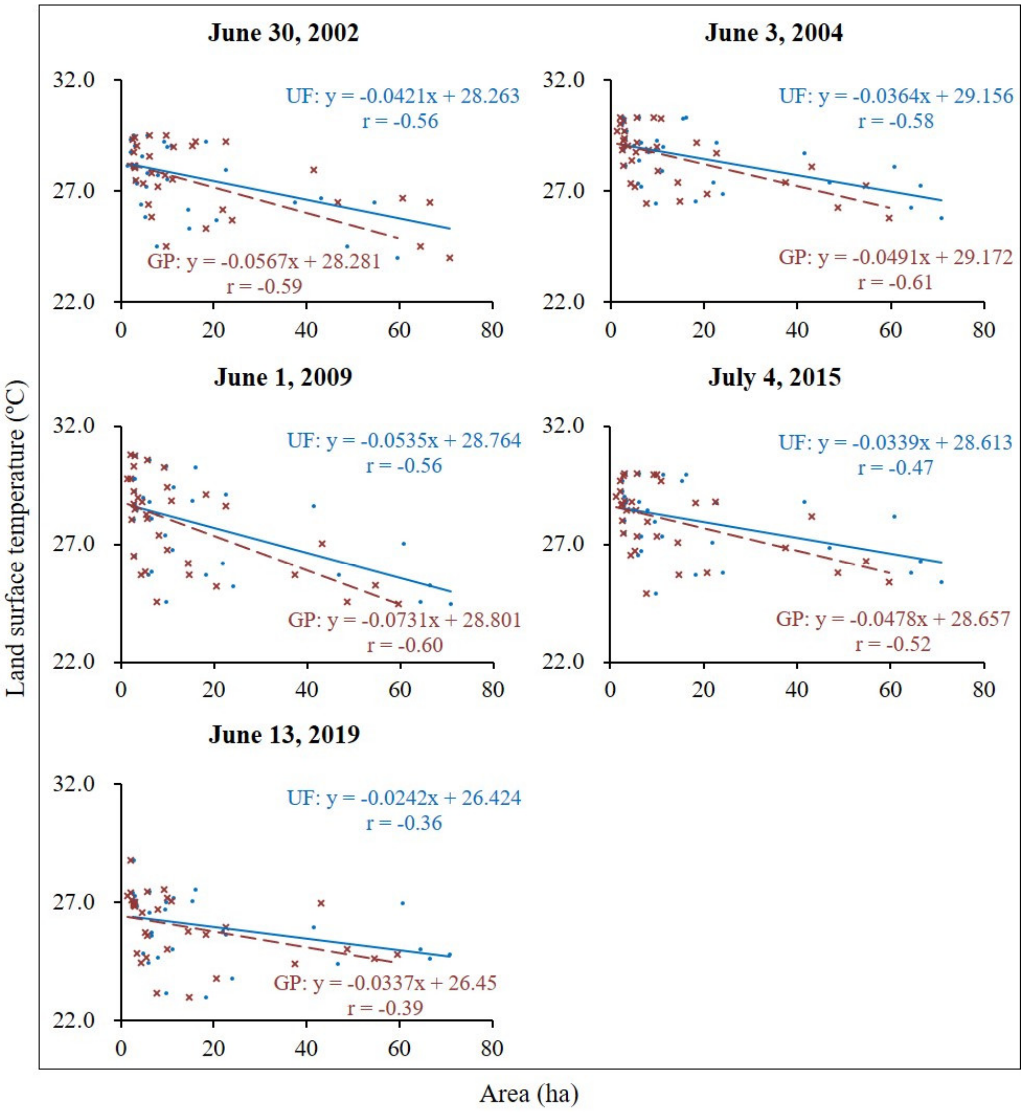

Figure 6. Comparison of two correlations (i) between the mean land surface temperatures (LSTs) in summer and urban forest size in area (UF—solid dots (•) with solid line (—) for the trend line in blue), and (ii) between the mean LSTs in summer and green patch size in area (GP—"×" marks with dashed line (- - -) for the trend line in red).

Due to the cooling effect of an urban forest, negative linear relationships were presented between the mean LSTs and urban forest sizes with Pearson's correlation r values ranging from −0.36 to −0.58, and green patch sizes with the r values from −0.39 to −0.61 (Figure 6). Due to the stronger correlation found between the LST and green patch size than urban forest size, it was considered that the cooling effect of an urban forest was better explained by the size of vegetation covered within urban forest than the urban forest size per se. To examine the cooling effect of the green patch size within an urban forest on its surrounding areas, urban forests were re-grouped by green patch size. The time-series changes in the LST of an urban forest and its buffers by green patch size are presented in Figure 7.

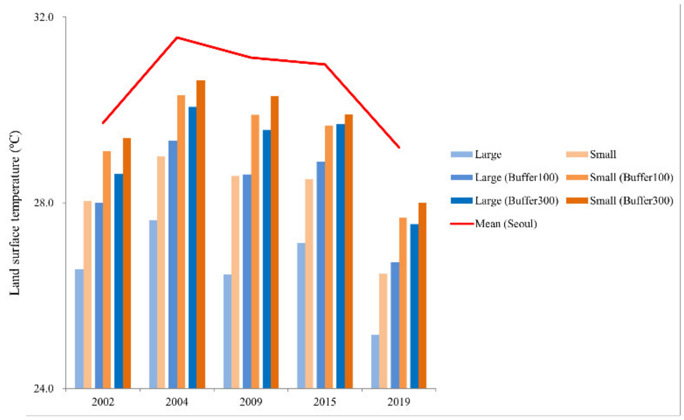

Figure 7. Comparison of spatiotemporal changes in mean land surface temperature (LST) between urban forest distinguished by green patch size and neighboring areas by buffer during the study period: one with green patch size smaller than 10 ha (small, in orange); the other with green patch size larger than 10 ha (large, in green). Average LST of Seoul is shown in red.

The 'large' group showed significantly lower mean LSTs than the 'small' group ($p \le 0.05$) (Figure 7). As for the 'large' group, urban forests indicated a significantly lower LST than $Buffer_{100}$ ($p \le 0.05$), the 'small' group of showed a similar pattern ($p \le 0.05$) (Figure 7). The mean LSTs of the 'large' group were significantly lower than those of Seoul ($p \le 0.05$), and those of the 'small' group were significantly lower than those of Seoul ($p \le 0.05$) (Figure 7). Considering the strong correlation of NDVI to the mean LST compared to urban forest size and green patch size (Table 3), a degree of green within the urban forest could be a reliable factor for estimating the cooling effect of urban forests. To investigate the relationship between greenness of urban forests and LST, correlation analysis was conducted in time-series between mean NDVI and mean LST for the individual urban forest (Figure 8).

Negative and strong linear relationships were found between the mean LST and mean NDVI with the r values ranging from −0.42 to −0.93 (Figure 8). The mean LST was reduced as the mean NDVI increased (Figure 8). Based upon the result in Figure 7 which suggested the cooling effect of urban forests could be explained from the size of green patch [38–40] and the result in Figure 8 where the NDVI showed a fairly strong correlation with LST [41–43], the mean NDVI of the urban forests with different green patch sizes were compared among themselves (Figure 9).

In both the 'small' and 'large' groups, the urban forests that showed a cooler mean LST showed a higher mean NDVI than those that showed a warmer mean LST during the entire study period in a consistent manner (Figure 9). It was considered that NDVI can be used for estimating the cooling capacity of urban forests.

To investigate if NDVI could be used for tracing the cooling capacity of urban forests which have been and/or would be undergoing forest dynamics over time, Seoul Forest was selected for time-series analyses. This site was once used as a racetrack and underwent overall destruction and re-development into an urban forest from the winter of 2003 to the spring of 2005. The completion of the redevelopment to a new large green space in the city was in the summer of 2005. The time-series mean LST and NDVI of Seoul Forest (UF SF) and those of the selected urban forests (UF 01 to UF 33) were compared to each other (Figure 10).

Compared to the group of the selected urban forests (UF 01 ~ UF 33), Seoul Forest showed relatively higher mean LST and lower mean NDVI in 2002 and 2004 (Figure 10a). There was a noticeable decrease in LST in Seoul Forest as the NDVI increased after 2009 (Figure 10a). Considering such a decrease in LST followed by improved NDVI, the cooling effect of an urban forest could be evaluated by NDVI.

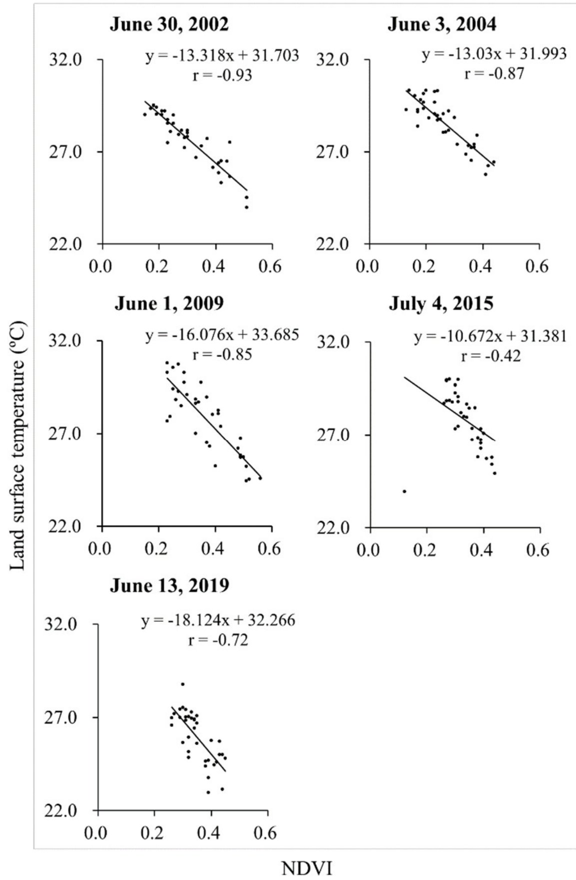

Figure 8. Temporal pattern in the correlations between the mean land surface temperatures (LSTs) and the mean NDVI for the urban forests in Seoul, from 2002 to 2019.

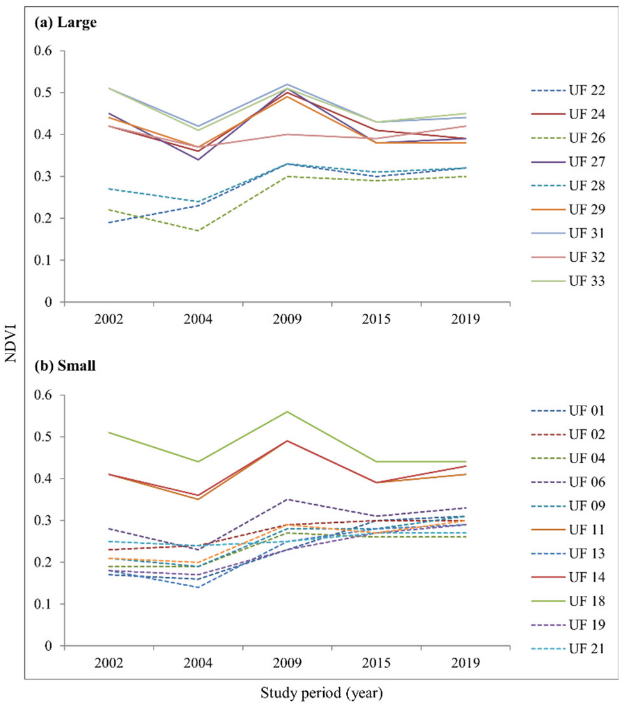

Figure 9. (**a**) Mean NDVI of the urban forests in the 'large' group which showed higher (dotted line) and lower (solid line) mean land surface temperatures (LSTs) than those of the entire urban forests in the group, and (**b**) mean NDVI of the urban forests in the 'small' group which showed higher (dotted line) and lower (solid line) mean LSTs than those of the entire urban forests in the group.

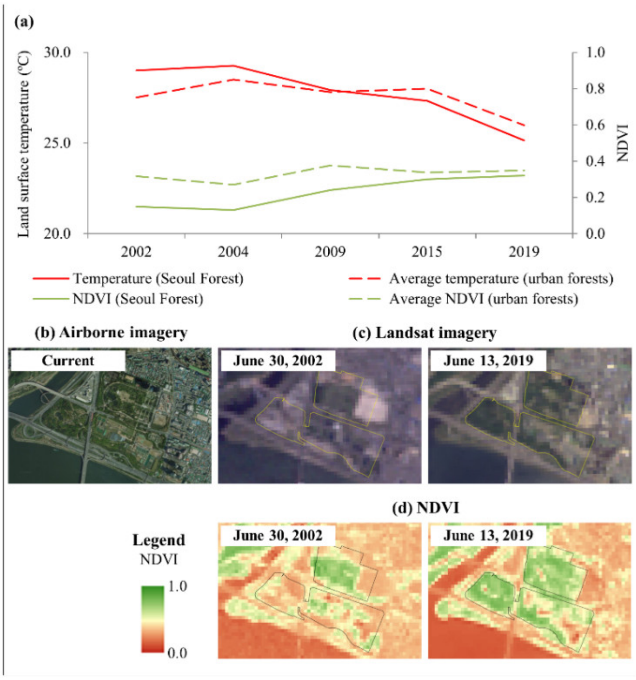

Figure 10. (**a**) Mean land surface temperature (LST) and NDVI of Seoul Forest and the group of the selected urban forests (UF 01 to 33) from 2002 to 2019, (**b**) airborne imagery of Seoul Forest, (**c**) Landsat imagery (true color) of Seoul Forest and its administrative boundary (in solid yellow) in 2002 and 2019, and (**d**) NDVI of Seoul Forest and its administrative boundary (in solid black).

4. Discussion

4.1. Cooling Effect of Urban Forest

To identify the influence range of urban forests towards surrounding areas in terms of cooling effect, LSTs of individual and groups of urban forests and their neighboring buffers were investigated. In general, urban forests showed lower LST compared to surrounding areas, and the changes in LST across the buffer regions presented that the cooling effect of the selected urban forests extends beyond the outer edge of the urban forests. This result corresponded to the results in earlier case studies on the cooling effect of urban forests with regards to distance from the urban forest. The LST increased gradually as the distance from the urban forest increased, and the cooling effect of the urban forest extended up to 300 m and 350 m in the previous studies [44,45]. In the study of Skoulikaa et al. [46], the LST tended to increase up to 300 m distance from the urban forest and stabilize at the range from 300 to 350 m beyond the park. Similarly, in our study, the result from investigating the cooling effect of urban forests indicated the point of inflection of about 300 m from the boundary of urban forest (Figures 3 and 4), although there were some sample sites which deviated from this general trend.

The use of Landsat imagery for the purpose of a spatiotemporally extensive time-series research involves three issues on data analysis and interpretation. Firstly, as the spatial resolutions of thermal infrared sensors (TIR) of Landsat 5 and 8 are 120 m and 100 m, respectively [31,47], it is not fully sufficient yet to fit our buffer regime that has a 100 m interval. As this study should cope with three critical conditions of satellite imagery which are large spatial coverage, multi-bands provision including thermal infrared, and the availability of time-series analysis, it was a challenge to make all the data sets and conditions fit for this design this time. The second issue is the possibility of mixing spatial information between two different neighboring features, which is partially related to the first issue above. As based on the set-up of the spatial unit, data analysis, and interpretation are affected, it is important to design how to deal with the areas where a feature adjoins the other. In the case that a forested patch could invade a non-forest area, the cooling effect of an urban forest might be exaggerated or underestimated. The impact range in this study, however, would be sustained because it was on the basis of pattern analysis. Lastly, the availability of Landsat imagery is in general limited at a certain time for our study area, and the acquisition time at 11 am local time is not the moment when neither the UHI effect nor the cooling effect is maximized or effectively observed. Fortunately, despite not using the data in the climax, it is considered identified patterns in this study positively meaningful. Nevertheless, future study can improve the outcome with more accuracy and precision by selecting different or additional available data sets and/or developing a more practical and effective approach.

4.2. Factors for the Cooling Effect

There is much research on the impact of the characteristics of land use and land cover (LULC) on the LST change in an urban area [48–51]. In this study, LULC which were the size of the whole urban forest, the size of vegetation cover within the urban forest or green patch, NDVI of the urban forest, and major types of land use in $Buffer_{100}$ and $Buffer_{300}$ were examined, but the result from the correlation analysis was not so significant (Table 4).

According to the correlation analysis between the mean LST of an urban forest and the major land-use types within $Buffer_{100}$ and $Buffer_{300}$, it was found that land use did not play a critical role in the thermal environment (Table 4). Rather, the LST of the urban forest tended to decrease, followed by increased urban forest size and green patch size, and improved NDVI of urban forests in general (Table 3; Figures 5 and 6). Based upon the stronger negative correlation that the LST showed against the green patch area and NDVI than urban forest size, it was considered that it could be more reliable to use vegetation-involved characteristics of an urban forest for estimating the cooling effect of urban forests. A similar suggestion was discussed in earlier studies with regards to the cooling effect with canopy density of vegetation distributed within urban forests. Whereas Jonsson [52] found urban forests containing dense vegetation showed relatively lower LST and quicker cooling rate than those containing sparse vegetation, Murphy et al. [53] and Ali and Patnaik [54] discovered ambient temperature of the urban forest tended to decrease followed by the increased proportion of vegetation cover and tree canopy density within the urban forest. Such relationships between the cooling effect of urban forests and vegetation-involved factors were well-reflected in spatiotemporal changes in LST in this study. The areas in close proximity to urban forests were under the influence of the cooling effect of the urban forests, and the cooling effect was more conductive where the land area of vegetation cover within the urban forest was larger (Figure 7). However, regardless of the differences in the vegetation coverage within urban forests, the LSTs were lower in the urban forests where NDVI was higher (Figure 9). It was considered that the cooling effect of urban forest on surrounding areas could be more affected by the condition of the vegetation within urban forests such as vegetation greenness and healthiness.

Table 4. Correlation analysis between the land surface temperature (LST) of urban forest and a suite of variables in relation to vegetation cover and major land use near the urban forest.

Dependent Variable	Independent Variable										
	UF [b]	**Green** [c]	**NDVI** [d]	**100G** [e]	**100R** [f]	**100C** [g]	**100T** [h]	**300G** [i]	**300R** [j]	**300C** [k]	**300T** [l]
Temp [a]	−0.44 **	−0.47 **	−0.78 **	−0.39 **	−0.30 **	0.14	−0.22 **	−0.41 **	−0.18 *	0.03	−0.18 *

※ **Descriptions for land use and land cover (LULC)**

- Forest and open space (green patch): Forest, grassland, paddy field, field, equipped farmland, orchard, nursery garden, planted area, cemetery, golf course, botanical garden, ancient palace, historical remain, and small-scale sports facility.
- Residential area: Detached house and apartment house.
- Commercial area: Commercial area and business area.
- Transportation facilities area: Railroad, road, and airport area.

*: $p \leq 0.05$, **: $p \leq 0.01$. [a]: Mean land surface temperature (LST) of urban forests in this study. [b,c,d]: Mean urban forest size, green patch size, and NDVI of the urban forest. [e,f,g,h]: Proportion of green patch, residential area, commercial area, transportation facilities area less than 100 m from the urban forest boundary ($Buffer_{100}$). [i,j,k,l]: Proportion of green patch, residential area, commercial area, transportation facilities area between 100 m and 300 m out of the urban forest boundary ($Buffer_{300}$).

4.3. Verification Case Analysis

Based upon this finding with regards to the condition of vegetation cover, a case study was conducted on Seoul Forest, which has experienced a major shift in its surface condition from a barren to a vegetated setting. Prior to the completion of redevelopment into the large city park in 2005, Seoul Forest showed higher LST than the average of the other urban forests while its NDVI was below 0.2 which indicates that there was no vegetation or was the lowest possible density of green leaves on-site [35]. However, after the completion of redevelopment, the LST decreased as NDVI of Seoul Forest increased. Considering that NDVI is an amenable tool used for estimating vegetation greenness, healthiness, and/or density [36], such a tendency at the Seoul Forest could attribute to the improved condition of vegetation cover over time. In addition, as the LST models in this study were developed solely relying on remotely sensed data rather than the field measurement, further validation is needed for a more reliable outcome [55–57].

5. Conclusions

This study investigated the cooling effect of the urban forest on its surrounding areas and the effective vegetation characteristics of urban forest for cooling the environment. By examining spatiotemporal changes in the urban thermal environment with different vegetation characteristics of urban forests, this study led to the conclusions as follows: (i) urban forest is cooler than surrounding areas, and in general cools down the LST of its surrounding areas, (ii) the size of the urban forest is not the prime factor for the cooling effect, but the vegetation greenness can be more related to the effect, and therefore (iii) NDVI could be a reliable manner to estimate the cooling capacity that urban forest contains. This study proceeded mainly in the use of the estimates of LST of the study area, not the measurements obtained on-site. Nevertheless, due to the correspondence of the findings in this study to previous studies, it is expected that our findings here could be useful for effectively developing urban forest plan and/or management.

Author Contributions: Conceptualization, P.S.-H.L.; methodology, P.S.-H.L. and J.P.; software, P.S.-H.L. and J.P.; validation, P.S.-H.L. and J.P.; formal analysis, P.S.-H.L. and J.P.; investigation, P.S.-H.L. and J.P.; resources, P.S.-H.L. and J.P.; data curation, P.S.-H.L. and J.P.; writing-original draft preparation, P.S.-H.L. and J.P.; writing-review and editing, P.S.-H.L.; visualization, P.S.-H.L. and J.P.; supervision, P.S.-H.L..; project administration, P.S.-H.L.; funding acquisition, P.S.-H.L.; All authors have read and agreed to the published version of the manuscript.

Funding: This work was supported by the National Research Foundation of Korea (NRF) grant funded by the Korean government (Ministry of Science and ICT) (No. NRF-2017R1C1B5017787).

Conflicts of Interest: The authors declare no conflict of interest.

References

1. Oke, T.R. The energetic basis of urban heat island. *Q. J. R. Meteorol. Soc.* **1982**, *108*, 1–24, doi:10.1002/qj.49710845502.
2. Bokaie, M.; Shamsipour, A.; Khatibi, P.; Hosseini, A. Seasonal monitoring of urban heat island using multi-temporal Landsat and MODIS images in Tehran. *Int. J. Urban Sci.* **2019**, *23*, 269–285, doi:10.1080/12265934.2018.1548942.
3. Sahana, M.; Dutta, S.; Sajjad, H. Assessing land transformation and its relation with land surface temperature in Mumbai city, India using geospatial techniques. *Int. J. Urban Sci.* **2019**, *23*, 205–225, doi:10.1080/12265934.2018.1488604.
4. Lee, P.; Jeong, J. Influence of vegetationi cover in Seoul Forest on PM10 concentration in Seoul, South Korea. *Asia Life Sci.* **2019**, *18*, 1–11.
5. Kolokotroni, M.; Zhang, Y.; Watkins, R. The London Heat Island and building cooling design. *Sol. Energy* **2007**, *81*, 102–110, doi:10.1016/j.solener.2006.06.005.
6. Frayssinet, L.; Merlier, L.; Kuznik, F.; Hubert, J.; Milliez, M.; Roux, J. Modeling the heating and cooling energy demand of urban buildings at city scale. *Renew. Sustain. Energy Rev.* **2017**, *81*, doi:10.1016/j.rser.2017.06.040.

7. Hassid, S.; Santamouris, M.; Papanikolaou, N.; Linardi, A.; Klitsikas, N.; Georgakis, C.; Asimakopoulos, D. Effect of the Athens heat island on air conditioning load. *Energy Build.* **2000**, *32*, 131–141, doi:10.1016/S0378-7788(99)00045-6.
8. Oke, T.R.; Crowther, J.; McNaughton, K.; Monteith, J.; Gardiner, B. The micrometeorology of the urban forest [and discussion]. *Philos. Trans. R. Soc. Lond. Ser. B Biol. Sci.* **1989**, *324*, 335–349.
9. Weng, Q.; Lu, D.; Schubring, J. Estimation of land surface temperature-vegetation abundance relationship for urban heat island studies. *Remote Sens. Environ.* **2004**, *89*, 467–483, doi:10.1016/j.rse.2003.11.005.
10. Stathopoulou, M.; Cartalis, C. Daytime urban heat islands from Landsat ETM+ and Corine land cover data. *Sol. Energy* **2007**, *81*, 358–368, doi:10.1016/j.solener.2006.06.014.
11. Cao, X.; Onishi, A.; Chen, J.; Imura, H. Quantifying the cool island intensity of urban parks using ASTER and IKONOS data. *Landsc. Urban Plan.* **2010**, *96*, 224–231, doi:10.1016/j.landurbplan.2010.03.008.
12. Li, X.; Zhou, W.; Ouyang, Z. Relationship between land surface temperature and spatial pattern of greenspace: What are the effects of spatial resolution? *Landsc. Urban Plan.* **2013**, *114*, 1–8, doi:10.1016/j.landurbplan.2013.02.005.
13. Oke, T.R. *Initial Guidance to Obtain Representative Meteorological Observations at Urban Sites*; IOM Report No.81, WMO/TD. No. 1250; World Meteorological Organization: Geneva, Switzerland, 2006.
14. Barsi, J.; Schott, J.; Hook, S.; Raqueno, N.; Markham, B.; Radocinski, R. Landsat-8 Thermal Infrared Sensor (TIRS) vicarious radiometric calibration. *Remote Sens.* **2014**, *6*, 11607–11626, doi:10.3390/rs61111607.
15. Xu, H.; Chen, B. Remote sensing of the urban heat island and its changes in Xiamen City of SE China. *J. Environ. Sci.* **2004**, *16*, 276–281.
16. Raissouni, N.; Sobrino, J. Toward remote sensing methods for land cover dynamic monitoring: Application to Morocco. *Int. J. Remote Sens.* **2000**, *21*, 353–366, doi:10.1080/014311600210876.
17. Wang, F.; Qin, Z.; Song, C.; Tu, L.; Karnieli, A.; Zhao, S. An improved mono-window algorithm for land surface temperature retrieval from Landsat 8 thermal infrared sensor data. *Remote Sens.* **2015**, *7*, 4268–4289, doi:10.3390/rs70404268.
18. Sobrino, J.; Jimenez-Munoz, J.; Paolini, L. Land surface temperature retrieval from LANDSAT TM 5. *Remote Sens. Environ.* **2004**, *90*, 434–440, doi:10.1016/j.rse.2004.02.003.
19. Qin, Z.; Karnieli, A.; Berliner, P. A mono-window algorithm for retrieving land surface temperature from Landsat TM data and its application to the Israel-Egypt border region. *Int. J. Remote Sens.* **2010**, *22*, 3719–3746, doi:10.1080/01431160010006971.
20. Cristóbal Rosselló, J.; Jimenez-Munoz, J.; Prakash, A.; Mattar, C.; Skoković, D.; Sobrino, J. An improved single-channel method to retrieve land surface temperature from the Landsat-8 thermal band. *Remote Sens.* **2018**, *10*, 431, doi:10.3390/rs10030431.
21. The Economist. Asian Green City Index: Assessing the Environmental Performance of Asia's Major Cities. 2011. Available online: https://eiuperspectives.economist.com/economic-development/asian-green-city-index/ (accessed on 3 February 2020).
22. Seoul Metropolitan Government. Seoul Population Census Data. 2019. Available online: https://data.seoul.go.kr/dataList/419/S/2/datasetView.do#/ (accessed on 3 February 2020).
23. Seoul Metropolitan Government. Topography of Seoul: Locations of Mountains and Rivers. 2005. Available online: https://parks.seoul.go.kr/ecoinfo/ecology/index.do/ (accessed on 3 February 2020).
24. Wybe, K. The nature of urban Seoul: Potential vegetation derived from the soil map. *Int. J. Urban Sci.* **2013**, *17*, 95–108, doi:10.1080/12265934.2013.766505.
25. Qiu, L.; Liu, F.; Zhang, X.; Gao, T. The reducing effect of green spaces with different vegetation structure on atmospheric particulate matter concentration in BaoJi city, China. *Atmosphere* **2018**, *9*, 332, doi:10.3390/atmos9090332.
26. Korean Ministry of the Interior and Safety. Street Address Background Map. 2020. Available online: http://www.juso.go.kr/addrlink/addressBuildDevNew.do?menu=layer/ (accessed on 31 January 2020).
27. Seoul Metropolitan Government. 2015 Urban Ecological Condition Survey Map. 2015. Available online: http://urban.seoul.go.kr/4DUPIS/sub7/sub7_7_4.jsp/ (accessed on 31 January 2020).
28. Choi, J.; Lee, S.; Ji, S.; Jeong, J.; Lee, P.S. Landscape analysis to assess the impact of development projects on forests. *Sustainability* **2016**, *8*, 1012, doi:10.3390/su8101012.
29. United States Geological Survey (USGS). EarthExplorer. 2019. Available online: https://earthexplorer.usgs.gov/ (accessed on 5 August 2019).

30. Avdan, U.; Jovanovska Kaplan, G. Algorithm for automated mapping of land surface temperature using LANDSAT 8 satellite data. *J. Sens.* **2016**, 1480307, doi:10.1155/2016/1480307.
31. United States Geological Survey (USGS). Landsat 8 Data Users Handbook Version 4.0. 2019. Available online: https://www.usgs.gov/land-resources/nli/landsat/landsat-8-data-users-handbook/ (accessed on 31 January 2020).
32. Sobrino, J.; Jimenez-Munoz, J.; Sòria Barres, G.; Romaguera, M.; Guanter, L.; Moreno, J.; Plaza, A.; Martinez, P. Land surface emissivity retrieval from different VNIR and TIR sensors. *Geosci. Remote Sens.* **2008**, *46*, 316–327, doi:10.1109/TGRS.2007.904834.
33. Sobrino, J.; Caselles, V.; Becker, F. Significance of the remotely sensed thermal infrared measurements obtained over a citrus orchard. *ISPRS J. Photogramm. Remote Sens.* **1990**, *44*, 343–354, doi:10.1016/0924-2716(90)90077-O.
34. Artis, D.A.; Carnahan, W.H. Survey of emissivity variability in thermography of urban areas. *Remote Sens. Environ.* **1982**, *12*, 313–329.
35. Weier, J.; Herring, D. *Measuring Vegetation (NDVI & EVI)*; NASA Earth Observatory: Washington, DC, USA, 2000. Available online: https://earthobservatory.nasa.gov/features/MeasuringVegetation/ (accessed on 31 January 2020).
36. Vermote, E.; Justice, C.; Claverie, M.; Franch, B. Preliminary analysis of the performance of the Landsat 8/OLI land surface reflectance product. *Remote Sens. Environ.* **2016**, *185*, 46–56.
37. Song, C.; Woodcock, C.; Seto, K.; Lenney, M.; Macomber, S. Classification and change detection using Landsat TM data: When and how to correct atmospheric effects? *Remote Sens. Environ.* **2000**, *75*, 230–244.
38. Vaz Monteiro, M.; Doick, K.; Handley, P.; Peace, A. The impact of greenspace size on the extent of local nocturnal air temperature cooling in London. *Urban For. Urban Green.* **2016**, *16*, 160–169, doi:10.1016/j.ufug.2016.02.008.
39. Gunawardena, K.; Wells, M.; Kershaw, T. Utilising green and bluespace to mitigate urban heat island intensity. *Sci. Total Environ.* **2017**, *584*, doi:10.1016/j.scitotenv.2017.01.158.
40. Zhang, Y.; Murray, A.; Turner, B.L. II. Optimizing green space locations to reduce daytime and nighttime urban heat island effects in Phoenix, Arizona. *Landsc. Urban Plan.* **2017**, *165*, 162–171, doi:10.1016/j.landurbplan.2017.04.009.
41. Deng, Y.; Wang, S.; Bai, X.; Tian, Y.; Wu, L.; Xiao, J.; Chen, F.; Qian, Q. Relationship among land surface temperature and LUCC, NDVI in typical karst area. *Sci. Rep.* **2018**, *8*, 641, doi:10.1038/s41598-017-19088-x.
42. Guha, S.; Govil, H.; Dey, A.; Gill, N. Analytical study of land surface temperature with NDVI and NDBI using Landsat 8 OLI and TIRS data in Florence and Naples city, Italy. *Eur. J. Remote Sens.* **2018**, *51*, 667–678, doi:10.1080/22797254.2018.1474494.
43. Bokaie, M.; Kheirkhah Zarkesh, M.; Daneshkar Arasteh, P.; Hosseini, A. Assessment of urban heat island based on the relationship between land surface temperature and land use/land cover in Tehran. *Sustain. Cities Soc.* **2016**, *23*, doi:10.1016/j.scs.2016.03.009.
44. Hamada, S.; Ohta, T. Seasonal variations in the cooling effect of urban green areas on surrounding urban areas. *Urban For. Urban Green.* **2010**, *9*, 15–24, doi:10.1016/j.ufug.2009.10.002.
45. Hamada, S.; Tanaka, T.; Ohta, T. Impacts of land use and topography on the cooling effect of green areas on surrounding urban areas. *Urban For. Urban Green.* **2013**, *12*, 426–434, doi:10.1016/j.ufug.2013.06.008.
46. Skoulika, F.; Santamouris, M.; Kolokotsa, D.; Boemi, N. On the thermal characteristics and the mitigation potential of a medium size urban park in Athens, Greece. *Landsc. Urban Plan.* **2014**, *123*, 73–86, doi:10.1016/j.landurbplan.2013.11.002.
47. United States Geological Survey (USGS). *Landsat—Earth Observation Satellites (Ver. 1.2, April 2020): U.S. Geological Survey Fact Sheet 2015–3081*; United States Geological Survey (USGS): Reston, VA, USA, 2016; 4p, doi:10.3133/fs20153081.
48. Carmona, P.; Tran, D.; Pla, F.; Myint, S.; Caetano, M.; Kieu, H. Characterizing the relationship between land use land cover change and land surface temperature. *ISPRS J. Photogramm. Remote Sens.* **2017**, *124*, 119–132, doi:10.1016/j.isprsjprs.2017.01.001.
49. Chaudhuri, G.; Mishra, N. Spatio-temporal dynamics of land cover and land surface temperature in Ganges-Brahmaputra delta: A comparative analysis between India and Bangladesh. *Appl. Geogr.* **2016**, *68*, doi:10.1016/j.apgeog.2016.01.002.
50. Jafari, R.; Hasheminasab, S. Assessing the effects of dam building on land degradation in central Iran with Landsat LST and LULC time series. *Environ. Monit. Assess.* **2017**, *189*, 74, doi:10.1007/s10661-017-5792-y.

51. Saha, P.; Bandopadhyay, S.; Kumar, C.; Mitra, C. Multi-approach synergic investigation between land surface temperature and land-use land-cover. *J. Earth Syst. Sci.* **2020**, *129*, 74, doi:10.1007/s12040-020-1342-z.
52. Jonsson, P. Vegetation as an urban climate control in the subtropical city of Gaborone, Botswana. *Int. J. Climatol.* **2004**, *24*, 1307–1322, doi:10.1002/joc.1064.
53. Murphy, D.; Hall, M.; Hall, C.; Heisler, G.; Stehman, S.; Anselmi-Molina, C. The relation between land cover and the urban heat island in northeastern Puerto Rico. *Int. J. Climatol.* **2011**, *31*, 1222–1239, doi:10.1002/joc.2145.
54. Ali, S.; Patnaik, S. Assessment of the impact of urban tree canopy on microclimate in Bhopal: A devised low-cost traverse methodology. *Urban Clim.* **2019**, *27*, 430–445, doi:10.1016/j.uclim.2019.01.004.
55. Chave, J.; Davies, S.; Phillips, O.; Lewis, S.; Sist, P.; Schepaschenko, D.; Armston, J.; Baker, T.; Coomes, D.; Disney, M.; et al. Ground data are essential for biomass remote sensing missions. *Surv. Geophys.* **2019**, *40*, 1–18, doi:10.1007/s10712-019-09528-w.
56. Sabol, D.; Gillespie, A.; Abbott, E.; Yamada, G. Field validation of the ASTER Temperature–Emissivity Separation algorithm. *Remote Sens. Environ.* **2009**, *113*, 2328–2344, doi:10.1016/j.rse.2009.06.008.
57. White, W.; Alsina, M.; Nieto, H.; McKee, L.; Kustas, W. Determining a robust indirect measurement of leaf area index in California vineyards for validating remote sensing-based retrievals. *Irrig. Sci.* **2018**, doi:10.1007/s00271-018-0614-8.